frontiers | Frontiers in Photonics

ORIGINAL RESEARCH
published: 25 July 2022
doi: 10.3389/fphot.2022.937622

Double-Pass Multiple-Plate Continuum for High-Temporal-Contrast Nonlinear Pulse Compression

Bo-Han Chen[1], Jia-Xuan Su[1], Jhan-Yu Guo[1], Kai Chen[2,3], Shi-Wei Chu[4,5], Hsuan-Hao Lu[6], Chih-Hsuan Lu[1] and Shang-Da Yang[1]**

[1]Institute of Photonics Technologies, National Tsing Hua University, Hsinchu, Taiwan, [2]Robinson Research Institute, Faculty of Engineering, Victoria University of Wellington, Wellington, New Zealand, [3]The Dodd-Walls Centre for Photonic and Quantum Technologies, Dunedin, New Zealand, [4]Department of Physics, National Taiwan University, Taipei, Taiwan, [5]Molecular Imaging Center, National Taiwan University, Taipei, Taiwan, [6]Elmore Family School of Electrical and Computer Engineering and Purdue Quantum Science and Engineering Institute, Purdue University, West Lafayette, IN, United States

We propose a new architecture, double-pass multiple-plate continuum (DPMPC), for nonlinear pulse compression. In addition to having a smaller footprint, a double-pass configuration is designed to achieve substantial bandwidth broadening without incurring noticeable higher-order dispersion, thus improving the temporal contrast over those of the traditional single-pass geometry when only the quadratic spectral phase can be compensated. In our proof-of-concept experiment, 187 μJ, 190-fs Yb-based laser pulse is compressed to 20 fs with high throughput (75%), high Strehl ratio (0.76), and excellent beam homogeneity by using DPMPC. The subsequently generated octave-spanning spectrum exhibits a significantly raised blue tail compared with that driven by pulses from a single-pass counterpart.

Keywords: ultrafast science, nonlinear optics, spectral broadening, supercontinuum generation, pulse compression

OPEN ACCESS

Edited by:
Paolo Bardella, Politecnico di Torino, Italy

Reviewed by:
Vassilios Kovanis, Virginia Tech, United States
Lifu Zhang, Shenzhen University, China

****Correspondence:***
Chih-Hsuan Lu
lzch2000@hotmail.com
Shang-Da Yang
shangda@ee.nthu.edu.tw

Specialty section:
This article was submitted to Light Sources and Luminescent Materials, a section of the journal Frontiers in Photonics

Received: *06 May 2022*
Accepted: *23 June 2022*
Published: *25 July 2022*

Citation:
Chen B-H, Su J-X, Guo J-Y, Chen K, Chu S-W, Lu H-H, Lu C-H and Yang S-D (2022) Double-Pass Multiple-Plate Continuum for High-Temporal-Contrast Nonlinear Pulse Compression. Front. Photonics 3:937622. doi: 10.3389/fphot.2022.937622

1 INTRODUCTION

Ti: Sapphire laser "dynasty" in ultrafast optics (Spence et al., 1991; Wirth et al., 2011) has lasted 3 decades primarily because of the superb time resolution (down to 5 fs) (Ell et al., 2001) and high pulse energy (up to 250 J). However, the short upper-state lifetime (3.2 μs) and the requirement of green pump result in low repetition rate and low average power, which are unpleasant in applications such as material processing and coincident measurement (Ullrich et al., 2003). Industrial-grade Yb-doped lasers have received increasing attention as a scientific research tool in recent years. In addition to compactness and robustness, the gain media have sub-millisecond upper-state lifetime and can be directly pumped by the diode to achieve high repetition rate (up to tens of MHz) and high average power (up to kilowatts). However, the relatively narrow gain bandwidth only supports sub-picosecond to picosecond pulses, leaving the applications based on few-cycle pulses still on the playground of Ti: Sapphire laser (Jeong et al., 2018).

A straightforward solution to improve the pulse width of industrial grade Yb-doped lasers is using a nonlinear pulse compressor. Various nonlinear pulse compression techniques, such as filamentation (Hauri et al., 2005; Zaïr et al., 2007), photonic-crystal fiber (PCF) (Ermolov et al., 2019; Köttig et al., 2020), hollow-core fiber (HCF) (Jeong et al., 2018; Nagy et al., 2019), multi-pass cell (Weitenberg et al., 2017; Lavenu et al., 2018; Ueffing et al., 2018), and multiple-plate continuum

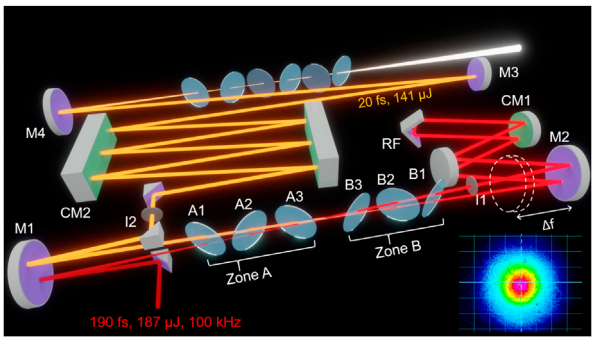

FIGURE 1 | Experimental setup of DPMPC. PM: pick-off mirrors; M#: concave mirrors; CM#: chirped mirror sets; I#: irises, A# and B#: quartz plates; RF: roof mirror; HRM: High-reflection mirror; Inset: beam profile taken after I2.

(MPC) (Lu et al., 2014, 2019; Beetar et al., 2018), have been explored and applied to metrology, time-resolved spectroscopy (Tamming et al., 2021), generation of coherent extreme ultraviolet (Huang et al., 2018), and terahertz radiation (Kanda et al., 2021). Filamentation is relatively easy to setup and can produce a broadband spectrum. However, the accompanied plasma generation often leads to extremely low transmission. PCF can also generate an extremely broad spectrum. The fiber geometry and the specially designed core structures allow good guiding effect and transmission with a rather low-loss. Yet, its low damage threshold usually limits the input energy to several μJ. HCF compressors can deliver exceptionally high pulse energy and beam quality, but are extremely sensitive to beam pointing fluctuation. Both the multi-pass cell and MPC implement spectral broadening in a cascaded fashion. The Multi-pass cell accumulates a small nonlinear phase shift φ_{NL} per pass, while the intensity is maintained by (chirped or unchirped) focusing mirrors. The overall spectral broadening (depending on the total φ_{NL}) can be large after many passes, and the resulting spectral shape is highly symmetric due to the distributed nature of nonlinear effect. However, the multi-pass cell requires special mirrors with a specific group-delay dispersion (GDD) over an octave-spanning bandwidth to achieve sub-10 fs pulses (Balla et al., 2020). Furthermore, the lengthy optical path caused by multiple bounces in the cell could be a trouble for temporal synchronization in pump-probe applications. In contrast, the traditional MPC pushes φ_{NL} close to the limit in each plate, while the risk of self-focusing-induced damage or wavefront distortion can be managed by adjusting the thicknesses of and distances between the plates. A Single-cycle pulse can be generated in a simple optical setup without the demanding alignment (Lu et al., 2014). The downside of MPC is the poorer temporal pulse contrast due to the asymmetric spectral shape (when self-steepening matters) coupled with the stronger higher-order dispersion. Customized chirped mirrors are often required to effectively remove the nonlinear chirp (Lu et al., 2019).

In this contribution, we demonstrate double-pass multiple-plate continuum (DPMPC), aiming to improve the temporal contrast of few-cycle MPC pulses in a compact setup. In this architecture, the moderately broadened spectrum and predominantly quadratic spectral phase after the first pass permit nearly perfect dispersion compensation by using off-the-shelf chirped mirrors with a constant GDD. The "well-behaved" output pulse resumes a self-phase modulation (SPM)-dominated spectral broadening in the second pass with the reduced higher-order dispersion. After the removal of linear chirp and the introduction of an additional MPC stage, we achieve an octave-spanning spectrum with a blue tail enhanced by ~10 dB.

2 EXPERIMENTAL SETUP AND RESULTS

Figure 1 shows the experimental setup of DPMPC. A Yb:KGW laser (Carbide, Light Conversion) delivers 190 fs, 187 μJ pulses at a 100 kHz repetition rate and a 1,030 nm central wavelength. A concave mirror M1 (f = 50 cm) focuses the beam onto a 200-μm-thick quartz plate to initiate the spectral broadening process, where the peak intensity is estimated to be 6.52 TW/cm^2. Two subsequent quartz plates with the same thickness are inserted behind the self-focused position from the previous plate, such that a maximal broadening can be achieved while no damage is observed (Lu et al., 2014). These three plates form "Zone A", after which no spectral broadening is observed by adding additional plates [dashed, **Figure 2A**.

After the first pass, an iris I1 is used to improve the beam homogeneity by blocking the rim with less spectral broadening. The pulse energy becomes 173 μJ, corresponding to 92.5% throughput. A second concave mirror M2 (f = 50 cm) is used to collect the diverging beam after Zone A. Note that the position of M2 is deliberately detuned from the cavity condition (by Δf = 20 mm) such that the beam is slightly converging instead of being collimated. A pair of chirped mirror CM1 and a retroreflector are employed to compensate the dispersion accumulated during the first optical pass (including all the six plates) and redirect the beam back to M2 at the same angle but at a lower position. The de-chirped pulse is characterized by polarization-gating frequency-resolved optical gating (PG-FROG). After 4 bounces of chirped mirrors (−2000 fs^2 in total), the pulse width (FWHM) is compressed to 54.2 fs [blue solid, **Figure 3A**] with 164 μJ energy and a Strehl ratio (peak power relative to that of a Fourier-limited pulse of the same energy) of 0.82. As the beam is slightly converging, the focal spot is moved closer to M2, where the peak intensity increases to ~20.1 TW/cm^2.

In order to avoid multiple filaments and optical breakdown, thinner (50 μm) quartz plates are used in Zone B. The plates are put in the same way as in Zone A, and the output beam is collected by M1, spatially filtered by I2, and guided to the second set of chirped mirror CM2 by a pick-off mirror. After 8 bounces of chirped mirrors (−480 fs^2 in total), pulse width is down to 20 fs [blue solid, **Figure 3C**] with 141 μJ energy (corresponding to throughputs of 89.5% and 75.4% for the second pass and the entire DPMPC system) and a Strehl ratio of 0.76, respectively.

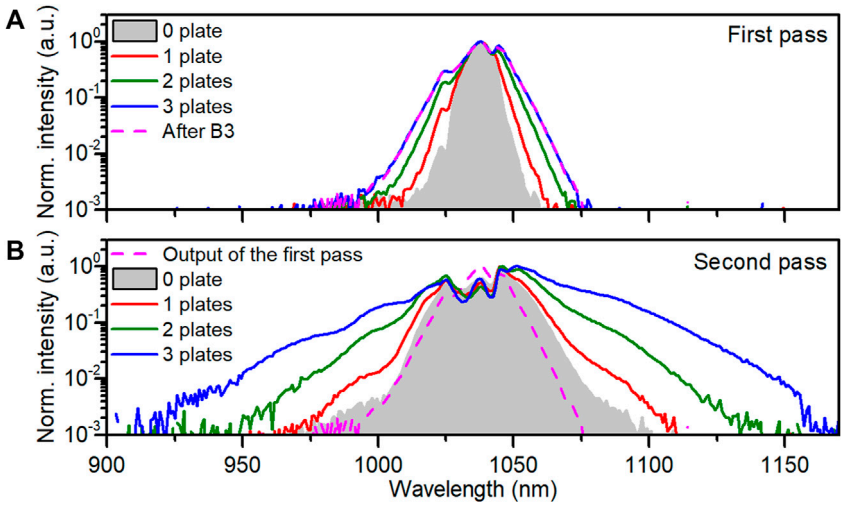

FIGURE 2 | Spectral evolution during the **(A)** first pass, and **(B)** second pass in DPMPC.

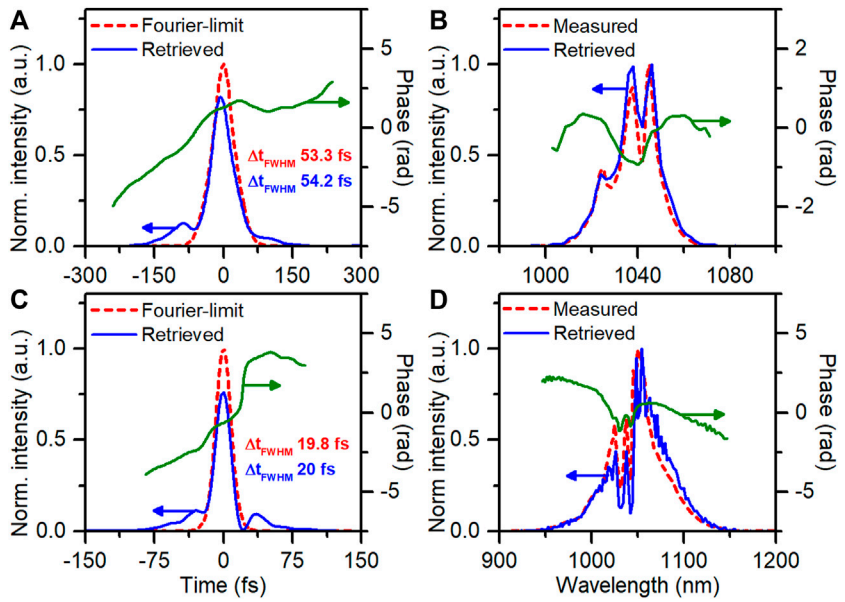

FIGURE 3 | PG-FROG measurement of pulses after the **(A,B)** first, and **(C,D)** second passes in **(A,C)** time, and **(B,D)** frequency domains, respectively. The retrieved intensity profiles in **(A)** and **(C)** are normalized to the energy of their Fourier-limit cases. FROG error: 0.36% for **(A,B)** and 0.51% for **(C,D)**.

Spectral evolutions during the two passes (**Figure 2**) exhibit the signatures of SPM, where the relatively symmetric shapes support the Fourier-limit pulses of higher temporal contrast [red dashed, **Figures 3A, C**] than those arising from self-steepening or white-light generation (Bradler et al., 2009). **Figure 2A** also confirms that the plates in Zone B do not disturb spectral broadening in the first pass, as the spectrum after plate B3 (dashed) resembles that after plate A3 (blue solid). Limited by the folded geometry, spectra in the second pass [**Figure 2B**] are measured after iris I2. Given the input spectrum (grey shaded) is slightly broader than the output spectrum of the first pass [blue, **Figure 2A**], plates in Zone A could have minor impact on spectral broadening in the second pass while no noticeable extra loss or beam deterioration is observed.

Figure 4 shows the spatially resolved power spectrum of DPMPC beam measured by acquiring the power spectrum after a 600-μm-wide slit scanning across the beam cross section. The 2D patterns exhibit virtually no tilted structure and the calculated homogeneity values V (Weitenberg et al., 2017) are higher than 87% within the 1/

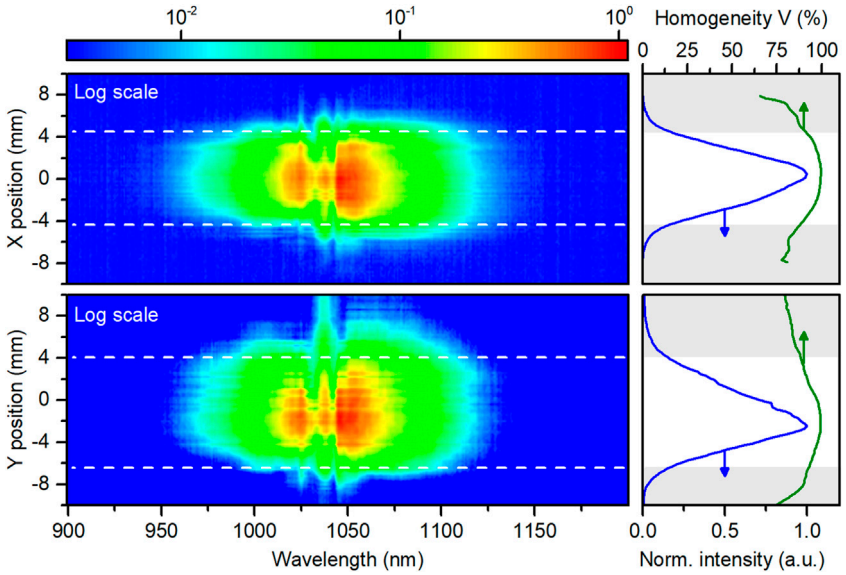

FIGURE 4 | Homogeneity measurement along x- and *y*-axis of the DPMPC beam. The white-dashed lines on the left panel define the borders where light intensity drops to $1/e^2$ of its peak.

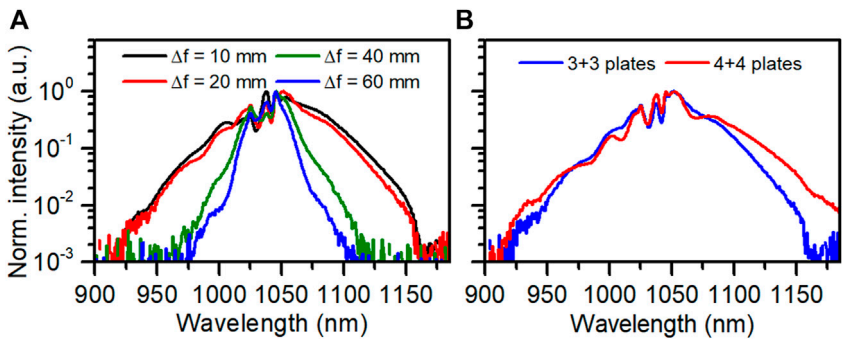

FIGURE 5 | Output spectra of DPMPC measured at different **(A)** M2 positions and **(B)** numbers of quartz plates.

e^2 diameter for both x- and *y*-axis, indicating good beam homogeneity. The beam caustic measurement (at 1,064 nm) also shows great beam quality with M_X^2 and M_Y^2 values 1.08 and 1.16, respectively.

The flexibility of DPMPC is experimentally verified in two aspects. First, output spectra are measured when the concave mirror M2 is deviated from the cavity condition by different amounts of Δf [**Figure 5A**]. For Δf < 10 mm, the back focal plane (where plate B1 is supposed to be placed) will be too close to Zone A, leaving insufficient space for Zone B. As Δf increases, the output spectrum is narrower because of the bigger focal spot size (thus lower peak intensity). Spectral broadening in the second pass would be nominal if Δf > 60 mm. This indicates that DPMPC can operate over a wide range of parameters without failure. Here we elect to operate at Δf = 20 cm, a condition which leaves us enough space for DPMPC while achieving the near-optimal spectral broadening [red, **Figure 5A**]. Second, we tried DPMPC with different amounts of plates (3 + 3 plates and 4 + 4 plates) at fixed Δf = 20 mm [**Figure 5B**]. As expected, the spectrum arising from 4 + 4 plates (red) is broader than the case of 3 + 3 plates (blue) owning to its longer interaction length (thus more total φ_{NL}). However, the resulting spectrum slightly exceeds the high reflection coating range of the optics (M1), causing the additional power loss after compression. Furthermore, the additional dispersion from the material requires more amount of GDD and even third-order dispersion (TOD) engineering for quality dispersion compression. As a result, we choose 3 + 3 plates for most of our demonstrations.

The advantage of DPMPC over the traditional single-pass geometry in terms of the subsequent octave-spanning spectrum generation is demonstrated in **Figure 6**. With the same input

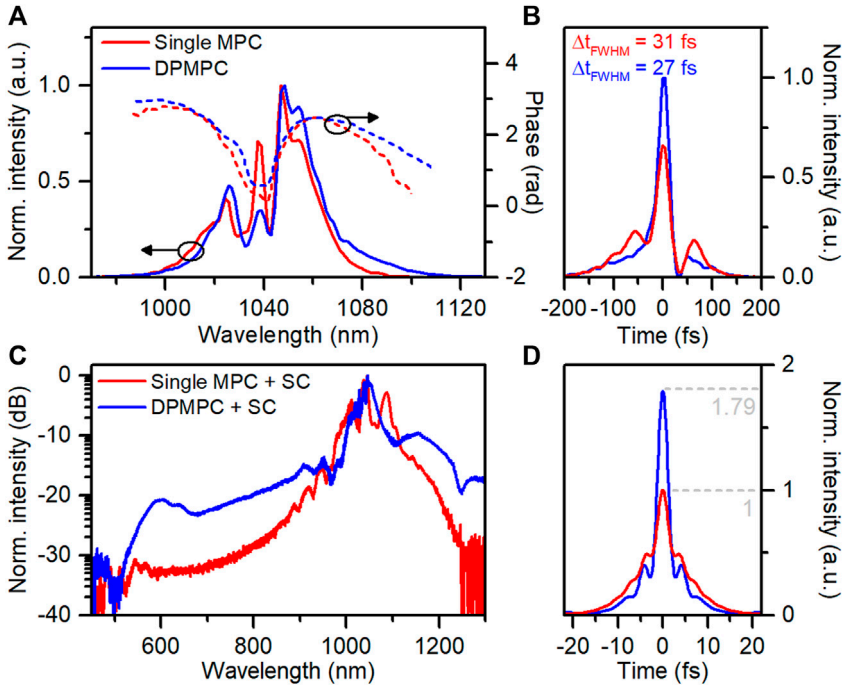

FIGURE 6 | (A,B) Pulses from single-pass MPC (red) and DPMPC (blue) retrieved by PG-FROG, where the areas under curves in **(B)** are proportional to the pulse energies. **(C)** The corresponding SC spectra generated in an extra MPC stage **(D)** The Fourier-limit temporal intensities (normalized to the same pulse energy) corresponding to the spectra in **(C)**.

pulse (190 fs, 187 μJ) and using six pieces of plates, both the techniques achieve supercontinuum (SC) [550–1,300 nm, **Figure 6C**] in the two stages (DPMPC + MPC and MPC + MPC). Since one single-pass MPC only manages to compress the input pulse to 31 fs [red, **Figure 6B**], the DPMPC is deliberately tuned to provide a similar pulse width [blue, **Figure 6B**] for fair comparison. The retrieved spectral phase curves [dashed, **Figure 6A**] show predominant quartic dependence, where the fitted fourth-order dispersion coefficient β_4 of single-pass MPC (2.7×10^6 fs^4) is 5 times larger than that of DPMPC (5.4×10^5 fs^4). The smaller residual β_4 of DPMPC supports a smoother pulse shape and a better temporal contrast [blue, **Figure 6B**], which are favorable for the subsequent SC generation. As shown in **Figure 6C**, the blue tail is enhanced by up to ~10 dB (at 600 nm). The more-symmetric spectral shape substantially suppresses the side peak level of the Fourier-limited pulse shape from 49% to 22% [**Figure 6D**], equivalent to the peak power enhancement by a factor of ~1.79 under the same pulse energy.

3 CONCLUSION

In summary, we propose and demonstrate DPMPC scheme to compress 100 kHz, 190 fs, 187 μJ pulses at 1,030 nm down to 20 fs with the high throughput (75%), high Strehl ratio (0.76), and good spatio-spectral homogeneity. The results show that an intermediate compression stage provides a well-behaved pulse that can resume a SPM-dominated spectral broadening with a less accumulation of higher-order dispersion. Pulses of high temporal contrast can arise after de-chirping by only using off-the-shelf chirp mirrors with a constant GDD. Such scheme promises a huge compression factor (9.5 in this work), making it an ideal tool for obtaining stable, high-power, few-cycle femtosecond laser pulses from industrial picosecond-level laser systems. This will help to reduce the heat affected zone during micro-machining processes, such as laser welding (Miyamoto et al., 2014, 2020). Subsequent SC generation shows that the blue spectral tail is enhanced by up to 10 dB. The enhanced spectral density in the visible makes DPMPC attractive in the spectroscopic investigation of photovoltaic materials (Li et al., 2019). With the proper dispersion management, single-cycle femtosecond pulses can be produced from the SC spectrum, which will provide an unprecedented temporal resolution for capturing extremely fast spectroscopic dynamics (Tamming et al., 2021; Ashoka et al., 2022).

DATA AVAILABILITY STATEMENT

The original contributions presented in the study are included in the article/Supplementary Material; further inquiries can be directed to the corresponding authors.

AUTHOR CONTRIBUTIONS

BC, CL, and SY contributed to the conception, designed the setup of the study, and wrote the manuscript. BC, JS, JG, and CL conducted the experiments and measurements. KC, SC, HL, and SY analyzed the results and discussed the research direction. All authors contributed to manuscript revision and read and approved the submitted version.

FUNDING

Funding was provided by the Ministry of Science and Technology of Taiwan (MOST 109-2112-M-007-013, MOST 109-2811-M-007-517, MOST 110-2811-M-007-508, and MOST 110-2321-B-002-012) and the BRC Research Center funding (110-2634-F-007-025).

REFERENCES

Ashoka, A., Tamming, R. R., Girija, A. V., Bretscher, H., Verma, S. D., Yang, S.-D., et al. (2022). Extracting Quantitative Dielectric Properties from Pump-Probe Spectroscopy. *Nat. Commun.* 13, 1–8. doi:10.1038/s41467-022-29112-y

Balla, P., Bin Wahid, A., Sytcevich, I., Guo, C., Viotti, A.-L., Silletti, L., et al. (2020). Postcompression of Picosecond Pulses into the Few-Cycle Regime. *Opt. Lett.* 45, 2572–2575. doi:10.1364/OL.388665

Beetar, J. E., Gholam-Mirzaei, S., Chini, M., and Chini, M. (2018). Spectral Broadening and Pulse Compression of a 400 μJ, 20 W Yb:KGW Laser Using a Multi-Plate Medium. *Appl. Phys. Lett.* 112, 051102. doi:10.1063/1.5018758

Bradler, M., Baum, P., Riedle, E., and Riedle, E. (2009). Femtosecond Continuum Generation in Bulk Laser Host Materials with Sub-μj Pump Pulses. *Appl. Phys. B* 97, 561–574. doi:10.1007/s00340-009-3699-1

Ell, R., Morgner, U., Kärtner, F. X., Fujimoto, J. G., Ippen, E. P., Scheuer, V., et al. (2001). Generation of 5-fs Pulses and Octave-Spanning Spectra Directly from a Ti:sapphire Laser. *Opt. Lett.* 26, 373–375. doi:10.1364/OL.26.000373

Ermolov, A., Heide, C., Dienstbier, P., Köttig, F., Tani, F., Hommelhoff, P., et al. (2019). Carrier-envelope-phase-stable Soliton-Based Pulse Compression to 44 Fs and Ultraviolet Generation at the 800 kHz Repetition Rate. *Opt. Lett.* 44 (20), 5005–5008. doi:10.1364/OL.44.005005

Hauri, C. P., Guandalini, A., Eckle, P., Kornelis, W., Biegert, J., and Keller, U. (2005). Generation of Intense Few-Cycle Laser Pulses through Filamentation - Parameter Dependence. *Opt. Express* 13, 7541–7547. doi:10.1364/OPEX.13.007541

Huang, P.-C., Hernández-García, C., Huang, J.-T., Huang, P.-Y., Lu, C.-H., Rego, L., et al. (2018). Polarization Control of Isolated High-Harmonic Pulses. *Nat. Phot.* 12, 349–354. doi:10.1038/s41566-018-0145-0

Jeong, Y. G., Piccoli, R., Ferachou, D., Cardin, V., Chini, M., Hädrich, S., et al. (2018). Direct Compression of 170-fs 50-cycle Pulses Down to 1.5 Cycles with 70% Transmission. *Sci. Rep.* 8, 11794. doi:10.1038/s41598-018-30198-y

Kanda, N., Ishii, N., Itatani, J., Matsunaga, R., and Matsunaga, R. (2021). Optical Parametric Amplification of Phase-Stable Terahertz-To-Mid-Infrared Pulses Studied in the Time Domain. *Opt. Express* 29, 3479. doi:10.1364/oe.413200

Köttig, F., Schade, D., Koehler, J. R., Russell, P. S. J., Tani, F., and Tani, F. (2020). Efficient Single-Cycle Pulse Compression of an Ytterbium Fiber Laser at 10 MHz Repetition Rate. *Opt. Express* 28, 9099–9110. doi:10.1364/OE.389137

Lavenu, L., Natile, M., Guichard, F., Zaouter, Y., Delen, X., Hanna, M., et al. (2018). Nonlinear Pulse Compression Based on a Gas-Filled Multipass Cell. *Opt. Lett.* 43, 2252. doi:10.1364/ol.43.002252

Li, M., Fu, J., Xu, Q., and Sum, T. C. (2019). Slow Hot-Carrier Cooling in Halide Perovskites: Prospects for Hot-Carrier Solar Cells. *Adv. Mat.* 31, 1802486. doi:10.1002/adma.201802486

Lu, C.-H., Tsou, Y.-J., Chen, H.-Y., Chen, B.-H., Cheng, Y.-C., Yang, S.-D., et al. (2014). Generation of Intense Supercontinuum in Condensed Media. *Optica* 1, 400–406. doi:10.1364/OPTICA.1.000400

Lu, C.-H., Wu, W.-H., Kuo, S.-H., Guo, J.-Y., Chen, M.-C., Yang, S.-D., et al. (2019). Greater Than 50 Times Compression of 1030 Nm Yb:KGW Laser Pulses to Single-Cycle Duration. *Opt. Express* 27, 15638. doi:10.1364/oe.27.015638

Miyamoto, I., Cvecek, K., Okamoto, Y., and Schmidt, M. (2014). Internal Modification of Glass by Ultrashort Laser Pulse and its Application to Microwelding. *Appl. Phys. A* 114, 187–208. doi:10.1007/s00339-013-8115-3

Miyamoto, I., Cvecek, K., and Schmidt, M. (2020). Advances of Laser Welding Technology of Glass-Science and Technology-. *J. Laser Micro/Nanoengineering* 15 (2), 63–76. doi:10.2961/jlmn.2020.02.1001

Nagy, T., Hädrich, S., Simon, P., Blumenstein, A., Walther, N., Klas, R., et al. (2019). Generation of Three-Cycle Multi-Millijoule Laser Pulses at 318 W Average Power. *Optica* 6, 1423. doi:10.1364/optica.6.001423

Spence, D. E., Kean, P. N., and Sibbett, W. (1991). 60-fsec Pulse Generation from a Self-Mode-Locked Ti:sapphire Laser. *Opt. Lett.* 16, 42–44. doi:10.1364/OL.16.000042

Tamming, R. R., Lin, C.-Y., Hodgkiss, J. M., Yang, S.-D., Chen, K., and Lu, C.-H. (2021). Single 3.3 Fs Multiple Plate Compression Light Source in Ultrafast Transient Absorption Spectroscopy. *Sci. Rep.* 11, 12847. doi:10.1038/s41598-021-92102-5

Ueffing, M., Reiger, S., Kaumanns, M., Pervak, V., Trubetskov, M., Nubbemeyer, T., et al. (2018). Nonlinear Pulse Compression in a Gas-Filled Multipass Cell. *Opt. Lett.* 43, 2070. doi:10.1364/ol.43.002070

Ullrich, J., Moshammer, R., Dorn, A., D rner, R., Schmidt, L. P. H., and Schmidt-B cking, H. (2003). Recoil-ion and Electron Momentum Spectroscopy: Reaction-Microscopes. *Rep. Prog. Phys.* 66, 1463–1545. doi:10.1088/0034-4885/66/9/203

Weitenberg, J., Vernaleken, A., Schulte, J., Ozawa, A., Sartorius, T., Pervak, V., et al. (2017). Multi-pass-cell-based Nonlinear Pulse Compression to 115 Fs at 75 MJ Pulse Energy and 300 W Average Power. *Opt. Express* 25, 20502–20510. doi:10.1364/OE.25.020502

Wirth, A., Hassan, M. T. H., Grguras, I., Gagnon, J., Moulet, A., Luu, T. T., et al. (2011). Synthesized Light Transients. *Sci.* 334, 195–200. doi:10.1126/science.1210268

Zaïr, A., Guandalini, A., Schapper, F., Holler, M., Biegert, J., Gallmann, L., et al. (2007). Spatio-temporal Characterization of Few-Cycle Pulses Obtained by Filamentation. *Opt. Express* 15, 5394–5405. doi:10.1364/OE.15.005394

Conflict of Interest: The authors declare that the research was conducted in the absence of any commercial or financial relationships that could be construed as a potential conflict of interest.

Publisher's Note: All claims expressed in this article are solely those of the authors and do not necessarily represent those of their affiliated organizations, or those of the publisher, the editors, and the reviewers. Any product that may be evaluated in this article, or claim that may be made by its manufacturer, is not guaranteed or endorsed by the publisher.